Int. J. Heat Mass Transfer. Vol. 13, pp. 471–490. Pergamon Press 1970. Printed in Great Britain

LAMINAR FORCED CONVECTION HEAT TRANSFER IN CURVED RECTANGULAR CHANNELS

K. C. CHENG and MITSUNOBU AKIYAMA
Department of Mechanical Engineering, University of Alberta, Edmonton, Alberta, Canada

(*Received* 17 *June* 1969 *and in revised form* 5 *September* 1969)

Abstract—The purpose of this paper is to present flow and heat transfer results obtained by a point successive over-relaxation method for steady fully developed laminar flow in curved rectangular channels under the thermal boundary conditions of axially uniform wall heat flux and peripherally uniform wall temperature at any axial position. The numerical method yields solutions up to a reasonably high Dean number for the aspect ratios $\gamma = 0{\cdot}2$, $0{\cdot}5$, 1, 2 and 5 considered in this study. It is noted that perturbation method is applicable only for relatively low Dean number region and boundary-layer technique is valid only for high Dean number regime.

Graphical results for $f\,Re/(f\,Re)_0$ and $Nu/(Nu)_0$, respectively, vs. Dean number are presented for $Pr = 0{\cdot}73$. Typical examples for axial velocity and temperature profiles, streamlines and velocity profiles for secondary flow and isotherms are also shown. For square channel, the effect of Prandtl number on heat transfer result is also investigated. Comparison of the result from this analysis and the result for high Dean number regime for the curved square channel available in the literature shows clearly that reasonable estimate can be made for the flow and heat transfer results for the Dean number ranging from 150 to 1000 where currently accurate solutions are not available.

NOMENCLATURE

a, width of a curved rectangular channel;
b, height of a curve rectangular channel;
C, constant, $C_1 D_e^3/4\nu\mu$;
C_1, axial pressure gradient, $-\partial P_0/\partial Z$;
C_2, axial temperature gradient, $\partial T/\partial Z$;
D_e, equivalent hydraulic diameter, $2ab/(a+b)$;
F_1, function defined in equation (12);
F_2, function defined in equation (15);
f, friction factor, $2\bar{\tau}_w/(\rho\bar{w}^2)$ or a dummy variable;
h, dimensionless grid spacing, $a/MD_e = b/2ND_e$;
$\bar{h}$, average heat transfer coefficient;
K, Dean number, $Re(D_e/R_c)^{\frac{1}{2}}$, see equation (21);
k, thermal conductivity;
M, number of divisions in X-direction;
N, number of divisions in Y-direction;
Nu, Nusselt number, $\bar{h}D_e/k$;
n, dimensionless inward-drawn normal or nth iteration for superscript;
P, pressure;
P_0, axial pressure distribution measured along the centerline and a function of Z only;
P', pressure deviation which is a function of X and Y only;
Pr, Prandtl number, ν/α;
R_c, radius of curvature of a curved rectangular channel;
Re, Reynolds number, $D_e\bar{W}/\nu$;
r_c, dimensionless radius of curvature of a curved rectangular channel, R_c/D_e;
T, local temperature;
T_w, wall temperature;
U, V, W, velocity components in X, Y and Z directions;
u, v, w, dimensionless velocity components in x, y and z directions;

X, Y, Z, Cartesian coordinates;
x, y, dimensionless Cartesian coordinates.

Greek letters

α, thermal diffusivity;
γ, aspect ratio of rectangular channel, a/b;
ε, a prescribed error;
θ, dimensionless temperature difference;
μ, viscosity;
ν, kinematic viscosity;
ξ, vorticity, $\partial V/\partial X - \partial U/\partial Y$;
ρ, density;
$\bar{\tau}_w$, mean shearing stress at wall;
ψ, dimensionless stream function;
ω, relaxation factor;
∇^2, dimensional or dimensionless Laplacian operator.

Subscripts

i, j, space subscripts of grid point in X and Y directions;
0, value for straight channel;
w, value at wall.

Superscripts

n, nth iteration;
$-$, average value.

1. INTRODUCTION

THE EFFECTS of body forces such as buoyancy, centrifugal, Coriolis and magnetic forces on flow and heat transfer characteristics in pipes or channels of various cross sectional shapes have been the subjects of many investigations in recent years. The forced convection problems with body force effect are frequently encountered in various heat exchangers, cooling or heating systems, reactors and heat engines. A number of combinations concerning the kind of body forces and the geometrical shape of the flow passages are possible in practical forced convective heat transfer problems. Trefethen [1] pointed out that secondary flow patterns in rotating radial tubes, heated horizontal tubes and curved tubes are qualitatively similar since the double helix secondary flows are caused by unbalanced body forces within the fluid.

Under certain conditions, a secondary flow due to body forces will not be established until a critical value of the characteristic parameter based on body force and the flow field is reached. The stability problem relating to the onset of the secondary flow has also attracted much attention in the past. For a flow in the curved rectangular channel, the critical value of the characteristic parameter (Dean number) is zero. The literature on flow and heat transfer in curved pipes is very extensive because of its technical importance. A literature survey and review of the pertinent works in this connection is given in [2]. In contrast to the number of published papers dealing with flow and heat transfer in curved pipes, the published works relating to flow and heat transfer in curved rectangular or other noncircular channels are rather limited in spite of its significance in practical applications.

The purpose of this work is to present an accurate numerical solution on forced convective heat transfer for steady fully developed laminar flow in curved rectangular channels with various aspect ratios under the thermal boundary conditions of axially uniform wall heat flux and peripherally uniform wall temperature at any axial position. Both Ito [3] and Cuming [4] presented theoretical analysis for flow in curved pipes of elliptic and rectangular sections using perturbation method. Dean and Hurst [5] obtained some analytical results for laminar flow in curved square channel by assuming uniform stream for secondary flow. Using boundary layer approximation along the wall, Ludwieg [6] presented analytical results for friction factors for fully developed laminar flow in helically coiled square channels rotating around its axis. Extensive experimental data covering both laminar and turbulent flows are compared against the theoretical results for laminar flow only with good agreement. Ex-

perimental results for friction factors are also presented for the case of stationary curved square channel with laminar and turbulent flows. Eichenberger [7] analysed entrance region problem in a curved rectangular channel with secondary flow by assuming an inviscid flow. Kapur *et al* [8] and Topakoglu [9] considered fully developed laminar flow in curved annuli. Experimental investigations on fully developed turbulent flows in a plane curved channel between concentric circular walls were reported by Wattendorf [10] and Eskinazi and Yeh [11] and turbulent heat transfer by Kreith [12]. Ustimenko *et al.* [13] presented flow and heat transfer results for fully developed laminar flow in curved flat channels with different ratios of heat fluxes at the inner and outer walls neglecting secondary flow effect.

Using boundary layer approximation, Mori and Uchida [14] presented analytical results for fully developed laminar flow in a curved square channel under the thermal boundary condition of axially uniform wall temperature gradient. Their results for flow and heat transfer are applicable only for the regime where Dean number is large. Velocity and temperature fields were obtained by dividing the cross section into core and boundary regions and considering the balances of kinetic energy and entropy production for the boundary layers. Mori and Uchida [15] also carried out theoretical investigation on forced convective heat transfer for fully developed laminar and turbulent flows in a curved channel under the condition of constant wall heat flux and compared the results with experimental measurements.

It is quite clear from the above brief review that more theoretical and experimental works are certainly required to bring our knowledge of flow and heat transfer in curved channels comparable to the level provided by the rather extensive data relating to flow and heat transfer in straight channels. It will be shown that the numerical method complements the boundary layer technique for high Dean number regime and yields accurate solution up to a reasonably high Dean number region for the aspect ratios $\gamma = 0{\cdot}2, 0{\cdot}5, 1, 2$ and 5 considered in this study.

2. FORMULATION OF THE PROBLEM

Consider a steady hydrodynamically and thermally fully developed laminar flow of viscous fluid in a curved rectangular channel under the thermal boundary conditions of axially uniform wall heat flux and peripherally uniform wall temperature at any axial position. The following assumptions are made in the analysis.

1. The radius of curvature of the rectangular channel is large compared with the hydraulic diameter of the cross-section of the channel.
2. Physical properties are constant.
3. Viscous dissipation is negligible.

Taking the origin of the rectangular coordinates (X, Y, Z) at the center of the rectangular cross-section as shown in Fig. 1 and applying

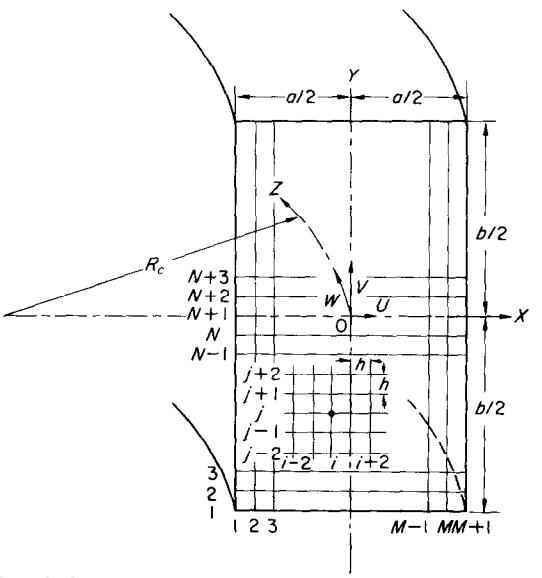

FIG. 1. Coordinate system and numerical grid for a curved rectangular channel.

the assumptions stated above, the governing equations for the present problem are;
Continuity Equation:

$$\frac{\partial U}{\partial X} + \frac{\partial V}{\partial Y} = 0, \tag{1}$$

Momentum Equation for Secondary Flow:

$$U\frac{\partial \xi}{\partial X} + V\frac{\partial \xi}{\partial Y} = \nu\nabla^2\xi - \frac{\partial}{\partial Y}\left(\frac{W^2}{R_c}\right), \quad (2)$$

where

$$\xi = \frac{\partial V}{\partial X} - \frac{\partial U}{\partial Y},$$

Axial Momentum Equation:

$$U\frac{\partial W}{\partial X} + V\frac{\partial W}{\partial Y} = -\frac{1}{\rho}\frac{\partial P_0}{\partial Z} + \nu\nabla^2 W, \quad (3)$$

Energy Equation:

$$U\frac{\partial T}{\partial X} + V\frac{\partial T}{\partial Y} + W\frac{\partial T}{\partial Z} = \alpha\nabla^2 T. \quad (4)$$

The pressure at any point consists of two parts as

$$P = P_0(Z) + P'(X, Y). \quad (5)$$

Boundary Conditions:

$$U = V = W = T - T_w = 0 \text{ at wall}$$
$$V = \frac{\partial U}{\partial Y} = \frac{\partial T}{\partial Y} = 0 \text{ along centerline } Y = 0. \quad (6)$$

Introducing the following transformations,

$$X = D_e x,\ Y = D_e y,\ R_c = D_e r_c,\ U = (\nu/D_e)v,$$
$$W = (\nu C/D_e)w,\ T - T_w = (C_2 D_e Pr C)\theta,$$
$$\partial P_0/\partial Z = -C_1, \partial T/\partial Z = C_2, C_1 D_e^3/4\nu\mu = C$$

where $D_e = 2ab/(a + b)$

and a dimensionless stream function ψ,

$$u = \partial\psi/\partial y, \qquad v = -\partial\psi/\partial x, \quad (7)$$

the governing equations may be restated in the following dimensionless forms.

Momentum Equation for Secondary Flow:

$$\frac{\partial\psi}{\partial y}\frac{\partial}{\partial x}\nabla^2\psi - \frac{\partial\psi}{\partial x}\frac{\partial}{\partial y}\nabla^2\psi = \nabla^2\nabla^2\psi + \frac{C^2}{r_c}\frac{\partial w^2}{\partial y}, \quad (8)$$

Axial Momentum Equation:

$$\frac{\partial\psi}{\partial y}\frac{\partial w}{\partial x} - \frac{\partial\psi}{\partial x}\frac{\partial w}{\partial y} = \nabla^2 w + 4, \quad (9)$$

Energy Equations:

$$Pr\left(\frac{\partial\psi}{\partial y}\frac{\partial\theta}{\partial x} - \frac{\partial\psi}{\partial x}\frac{\partial\theta}{\partial y}\right) = \nabla^2\theta - w. \quad (10)$$

Because of symmetry with respect to the X-axis, it is only required to consider the lower half of the rectangular cross-section (see Fig. 1). Consequently, the boundary conditions are:

$$\frac{\partial\psi}{\partial x} = \frac{\partial\psi}{\partial y} = w = \theta = 0 \text{ at channel wall}$$
$$\frac{\partial\psi}{\partial x} = \frac{\partial^2\psi}{\partial y^2} = \frac{\partial w}{\partial y} = \frac{\partial\theta}{\partial y} = 0 \quad (11)$$
along centerline $y = 0$.

The above set of equations constitutes a formal mathematical statement of the problem under consideration. In contrast to the forced convection problem with buoyancy effect, one notes that for the problem at hand, the momentum equations and the energy equation are uncoupled. It is possible to solve the above set of equations analytically by perturbation method as demonstrated in the literature for similar problems [3, 4], but the process is very tedious and the solution quickly diverges with the increase of the Dean number. In view of the considerable difficulties with the analytical method, the numerical solution using convergent iterative procedure will be presented in this study.

3. NUMERICAL SOLUTION

3.1 *Finite-difference approximation*

In recent years, finite-difference methods have been shown to be a powerful tool for the solution of natural convection problems [16–19]. Recently, Cheng and Hwang [20] presented numerical solution for fully developed combined free and forced laminar convection in horizontal rectangular channels using point successive-overrelaxation method. In this study, the point successive-overrelaxation method was further extended to solve a set of elliptic partial

differential equations and the associated boundary conditions. One notes that the axial momentum equation (9) may be regarded as

$$\nabla^2 w = F_1\left(u, v, \frac{\partial w}{\partial x}, \frac{\partial w}{\partial y}\right). \tag{12}$$

Using three-point central difference formula and square mesh, the finite-difference equation for equation (9) can be expressed as

$$w_{i,j} = \frac{1}{4}\left(w_{i+1,j} + w_{i-1,j} + w_{i,j+1} + w_{i,j-1}\right) - \frac{h^2}{4}\left\{u_{i,j}\frac{w_{i+1,j} - w_{i-1,j}}{2h} + v_{i,j}\frac{w_{i,j+1} - w_{i,j-1}}{2h} - 4\right\}. \tag{13}$$

Similarly, the finite-difference equation for the energy equation (10) becomes

$$\theta_{i,j} = \frac{1}{4}(\theta_{i+1,j} + \theta_{i-1,j} + \theta_{i,j+1} + \theta_{i,j-1}) - \frac{h^2}{4}\left\{Pr\left[u_{i,j}\frac{\theta_{i+1,j} - \theta_{i-1,j}}{2h} + v_{i,j} \times \frac{\theta_{i,j+1} - \theta_{i,j-1}}{2h}\right] + w_{i,j}\right\}. \tag{14}$$

To obtain the finite-difference equation for equation (8), one notes that this equation may be regarded as the inhomogeneous biharmonic equation in the following form.

$$\nabla^2\nabla^2\psi = F_2\left[\left(\frac{\partial}{\partial x}, \frac{\partial}{\partial y}\right)\psi, \left(\frac{\partial}{\partial x}, \frac{\partial}{\partial y}\right) \times \nabla^2\psi, w, \frac{\partial w}{\partial y}\right]. \tag{15}$$

Omitting the details, the finite-difference equation for the secondary flow stream function ψ at the mesh point (i, j) may be obtained by double application of the procedure transforming harmonic equation (12) into its finite-difference form. The result is

$$\begin{aligned}\psi_{i,j} = {} & \left(\frac{4}{10} - \frac{h}{10}u_{i,j}\right)\psi_{i+1,j} + \left(\frac{4}{10} + \frac{h}{10}u_{i,j}\right)\psi_{i-1,j} + \left(\frac{4}{10} - \frac{h}{10}v_{i,j}\right)\psi_{i,j+1} + \left(\frac{4}{10} + \frac{h}{10}v_{i,j}\right)\psi_{i,j-1} + \left(-\frac{1}{20} + \frac{h}{40}u_{i,j}\right)\psi_{i+2,j} + \left(-\frac{1}{20} - \frac{h}{40}u_{i,j}\right)\psi_{i-2,j} \\ & + \left(-\frac{1}{20} + \frac{h}{40}v_{i,j}\right)\psi_{i,j+2} + \left(-\frac{1}{20} - \frac{h}{40}v_{i,j}\right)\psi_{i,j-2} + \left(-\frac{1}{10} + \frac{h}{40}u_{i,j} + \frac{h}{40}v_{i,j}\right)\psi_{i+1,j+1} + \left(-\frac{1}{10} + \frac{h}{40}u_{i,j} - \frac{h}{40}v_{i,j}\right)\psi_{i+1,j-1} \\ & + \left(-\frac{1}{10} - \frac{h}{40}u_{i,j} + \frac{h}{40}v_{i,j}\right)\psi_{i-1,j+1} + \left(-\frac{1}{10} - \frac{h}{40}u_{i,j} - \frac{h}{40}v_{i,j}\right)\psi_{i-1,j-1} - \frac{h^3}{120}\left(\frac{C^2}{r_c}\right)w_{i,j} \\ & \times (-w_{i,j+2} + 8w_{i,j+1} - 8w_{i,j-1} + w_{i,j-2}).\end{aligned} \tag{16}$$

It is noted that for the derivative $\partial w/\partial y$ in equation (15), five-point difference formula is used. It suffices to note that five-point difference formula is used in computing secondary flow velocity components u, v from equation (7). For simplicity, the finite-difference expressions for the boundary conditions will be omitted except those along the horizontal center line $i = 1,2,\ldots M+1, j = N+1$. These are

$$w_{i,N} = w_{i,N+2}, \theta_{i,N} = \theta_{i,N+2}, \psi_{i,N} = -\psi_{i,N+2}, \psi_{i,N-1} = -\psi_{i,N+3}, \psi_{i,N+1} = v_{i,N+1} = 0.$$

It is well to note that the finite-difference expression for the stream function at the mesh point

next to the boundary takes special form after satisfying the boundary condition for ψ.

3.2 *Iterative method and point successive-over-relaxation method*

Point successive-overrelaxation method [21] is used in solving each differential equation. The iterative procedure employed is similar ro that used in [19, 20]. The detail of the procedure is given in [2]. The following test is used at the end of each iteration to determine the convergence of the computed function.

$$\text{Max} \left| f_{i,j}^{(n)} - f_{i,j}^{(n-1)} \right| / \max \left| f_{i,j}^{(n)} \right| < \varepsilon \quad (17)$$

where f is a dummy variable and ε is a prescribed error. Numerical experiment shows that the following prescribed errors are satisfactory.

$$\varepsilon_1 = 10^{-5} \quad \text{for } w_{i,j}, \psi_{i,j} \text{ and } \theta_{i,j}$$
$$\varepsilon_2 = 5 \times 10^{-5} \quad \text{for } u_{i,j} \text{ and } v_{i,j}.$$

The effects of grid size on computing time, and on flow and heat transfer results are studied in [2]. The round-off error is found to be negligible by using double precision in computation.

With the aspect ratio of the channel and Prandtl number given, numerical solution starts with Dean number $K = 0$ and proceeds gradually toward high Dean number regime. By increasing the Dean number and maintaining the same prescribed errors, the numerical solution is found to be convergent up to a reasonably high Dean number; but starting at a certain Dean number the secondary flow pattern changes from the regular two vortices to four vortices. The additional two weaker and smaller vortices are located near the central part of the outer wall. Numerical experiment also discloses the existence of a pair of solutions (2 vortices and 4 vortices) for a given Dean number in high Dean number regime. The conditions under which the double-solutions were encountered, and the details of the numerical experiment for secondary flow pattern with four vortices are described in [2]. Because of the uncertainties associated with the double-solutions, the flow and heat transfer results for the Dean number range with this peculiar behavior will not be presented.

When the magnitude of the secondary velocity components exceeds $2/h$, numerical results start oscillation for a solution with regular two vortices and finally the solution diverges. The above situation occurs at a certain high Dean number. One notes that the coefficient matrix is diagonally dominant when $|u_{i,j}|$ or $|v_{i,j}| \leqslant 2/h$. On the other hand, the numerical solution with four vortices is still convergent even when the Dean number far exceeds the value indicated above for the flow pattern with two vortices. Eventually, the numerical solution with four vortices also diverges when the magnitude of the secondary velocity components (u, v) exceeds $2/h$.

An example of computing time required may be of interest. It takes about 138 min by IBM 360/67 to obtain a complete result up to $C^2/r_c = 0{\cdot}17 \times 10^6$ for flow and heat transfer with $\gamma = 1$, $M = 32$, $N = 16$, and $Pr = 0{\cdot}71$.

To improve convergence in the process of iterations, a relaxation factor ω is used. The value of the factor ω usually lies between 1 and 2. A question naturally arises as to the optimum value of the factor ω_{op} that will yield a maximum rate of convergence. Unfortunately, no general method is available for the evaluation of the optimum relaxation factor for the elliptic-type partial differential equations with non-linear terms as encountered in the present problem. However, for the low Dean number region, one would expect that the method described in [21] may be applicable. In this study, the optimum relaxation factor ω_{op} for linear system is used when the Dean number is zero or sufficiently small. By using $\omega_{op} = 1{\cdot}75 \sim 1{\cdot}82$, considerable computing time is saved. For the Dean number ranging from small to intermediate values, different relaxation factors for equations (13), (14) and (16) are used after considerable numerical experiments. Some examples of relaxation factors used are given in [2]. One notes that in high Dean number region the relaxation factor $\omega = 1$ is found by trial and error to be the best value. Further details can be found in [2].

4. FLOW AND HEAT TRANSFER RESULTS

4.1 *Flow and heat transfer characteristics*

It is possible to obtain the expressions for the product of friction factor and Reynolds number, fRe, and the Nusselt number, Nu, by considering either the velocity and temperature gradients, respectively, along the channel wall or the overall force and energy balances, respectively for the axial length dZ. The results for resistance coefficient are

$$(fRe)_{\mathrm{I}} = \frac{2\left(\frac{\partial \overline{w}}{\partial n}\right)_w}{\overline{w}}, (fRe)_{\mathrm{II}} = \frac{2}{\overline{w}} \tag{18}$$

The Nusselt number is defined by

$$Nu = \frac{\overline{h} D_e}{k} \tag{19}$$

where $\overline{h}$ can be obtained in two ways. Using mixed mean temperature difference, the results are

$$(Nu)_{\mathrm{I}} = \frac{\left|\left(\frac{\partial \overline{\theta}}{\partial n}\right)_w\right| \overline{w}}{|(\overline{w\theta})|}, (Nu)_{\mathrm{II}} = \frac{\overline{w}^2}{4|(\overline{w\theta})|}. \tag{20}$$

The single or double integrations required for the evaluation of the mean values are carried out by using Simpson's rule. For the evaluation of the derivatives such as $(\partial \overline{w}/\partial n)_w$ and $(\partial \overline{\theta}/\partial n)_w$, five-point formula is found to be satisfactory. The foregoing two methods of evaluating (fRe) and Nu afford checking the accuracy of the numerical results. One notes that the Dean number can also be written as

$$K = \left(\frac{C^2}{r_c}\right)^{\frac{1}{2}} \overline{w}. \tag{21}$$

4.2 *The effect of Dean number on velocity and temperature fields*

In order to see the effect of Dean number on velocity and temperature fields, the dimensionless axial velocity and temperature profiles along the central horizontal axis $Y = 0$ and the vertical

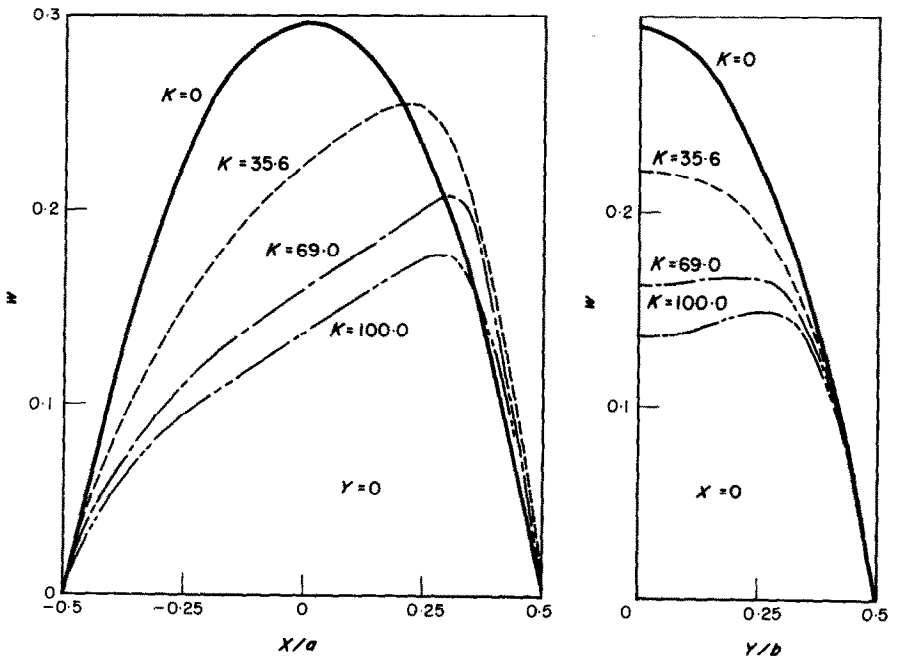

FIG. 2. Dimensionless axial velocity distribution in a curved square channel $\gamma = 1$ with K as a parameter.

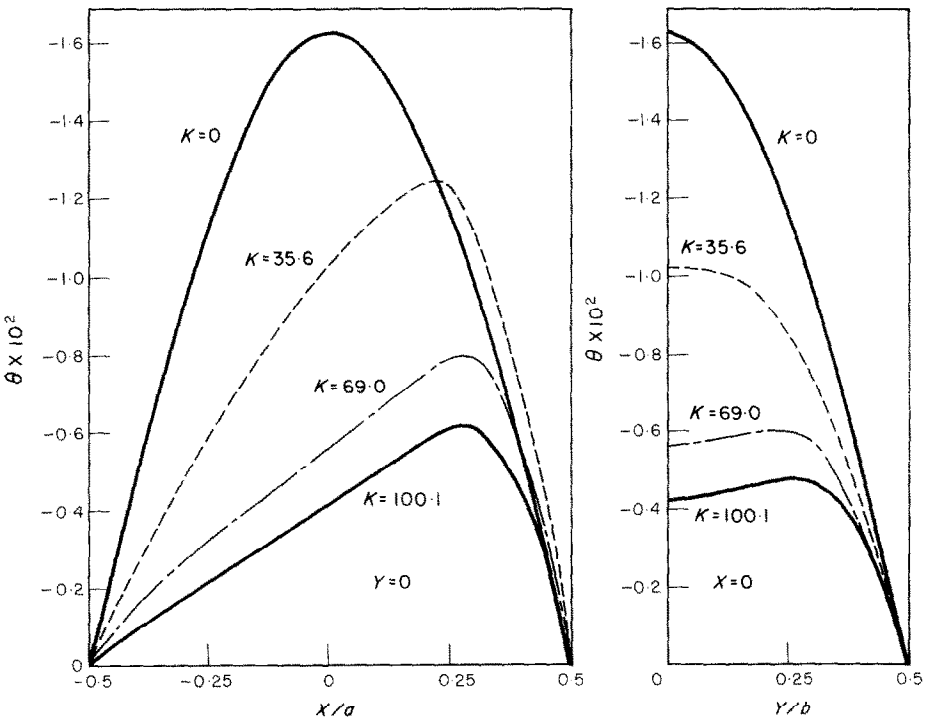

FIG. 3. Dimensionless temperature distribution in a curved square channel $\gamma = 1$ and $Pr = 0{\cdot}73$ with K as a parameter.

axis $X = 0$ are plotted for a curved square channel $\gamma = 1$ with $Pr = 0{\cdot}73$ for several representative Dean numbers in Figs. 2 and 3, respectively. Qualtitatively, the effect of centrifugal force on the flow and temperature fields are similar to the effect of buoyancy force for a given geometrical shape of channel and thermal boundary conditions at the wall. One can see clearly that the effect of the centrifugal force is to shift the location of the maximum value toward the outer wall and decrease the maximum value itself as the value of the Dean number increases. It is expected that the profiles for the velocity and temperature are similar.

Secondary flow streamlines and isothermals for a curved square channel are shown in Fig. 4 for $K = 51{\cdot}9$ and $Pr = 0{\cdot}73$. The location of the center of circulation is of interest since one can gain the general idea about the secondary flow pattern and the intensity of secondary flow. For a curved square channel, the X-coordinate of

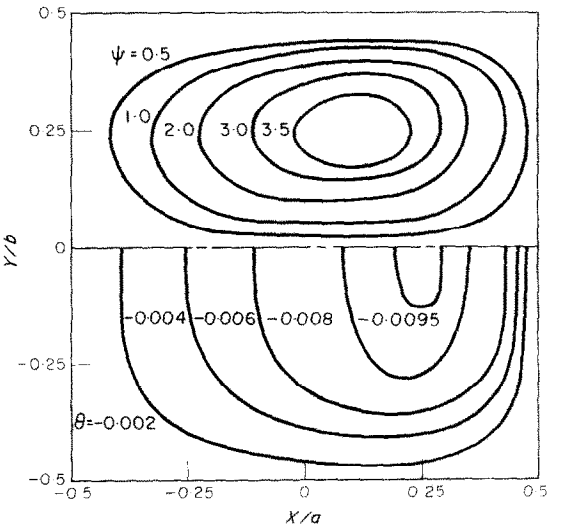

FIG. 4. Secondary flow streamlines and dimensionless isothermals for a curved square channel $\gamma = 1$ with $K = 51{\cdot}9$ and $Pr = 0{\cdot}73$.

the center of circulation gradually moves from $X/a = 0$ toward the outer wall as the Dean number increases and reaches about $X/a = 0{\cdot}1$ at $K = 45$. With further increase of the Dean number, the center of circulation tends to move back toward the center $X/a = 0$. It is found that with Dean number at about 125 the center of circulation returns to $X/a = 0$. On the other hand, with the increase of the Dean number, the Y-coordinate at the center of circulation always moves toward the upper or lower wall indicating increase of the intensity of secondary flow near the upper or lower wall.

The distributions of the secondary flow velocity components with the increase of the Dean number are also of considerable interest

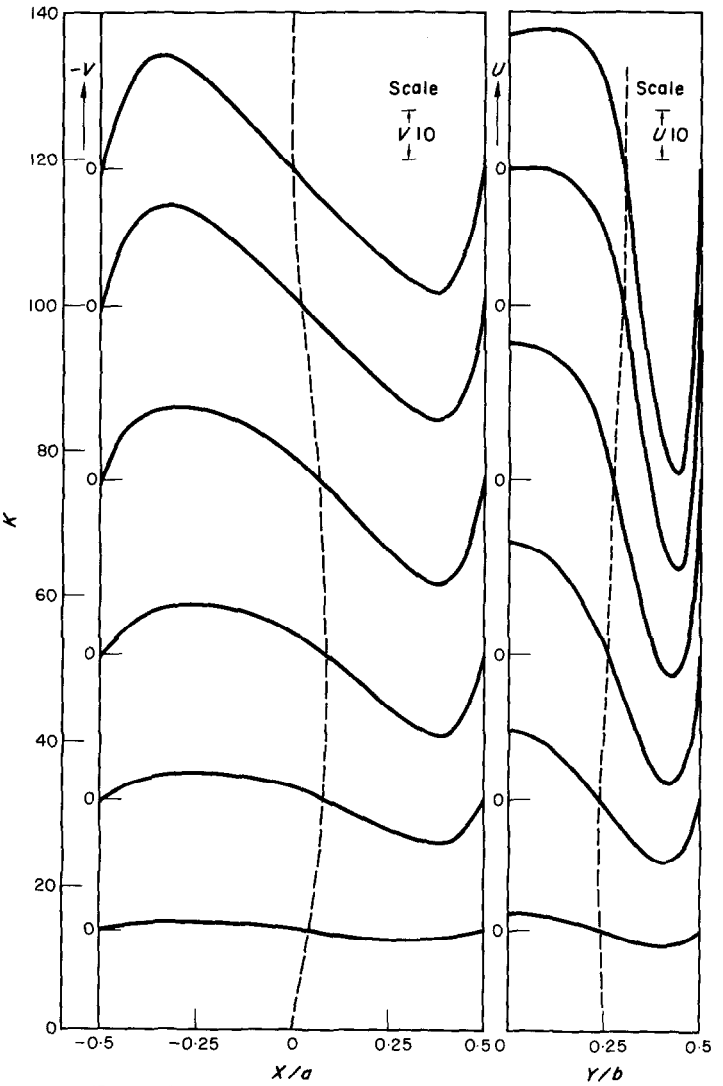

FIG. 5. Distribution of dimensionless secondary velocity components (u, v) in two directions (X and Y) passing through the center of circulation for a curved square channel $\gamma = 1$ with K as a parameter.

and these are shown in Fig. 5. One sees clearly the movement of the center of circulation along the broken lines with the increase of the Dean number in this figure. It is seen that the intensity of the secondary flow increases as the value of the Dean number increases.

The location of the maximum velocity point for a curved square channel is also of interest. At $K = 70$, the maximum velocity is located at around $X/a = 0{\cdot}28$ and seems to remain there with further increase of the Dean number. One may add that the location of the maximum value of the temperature profile shows exactly the same trend with $Pr = 0{\cdot}73$.

The distributions of velocity and temperature in Figs. 2 and 3 suggest that boundary layer approximation is possible for both velocity and temperature fields when the Dean number is high (see Fig. 5). This observation is important since it confirms the applicability of the boundary layer approximation for the high Dean number region [14].

One can gain some insight into the flow pattern in a curved rectangular channel by considering the distribution of centrifugal forces and pressure in a cross-section. For a given radius of curvature, the centrifugal force is proportional to the square of the axial velocity at a given point and acting in a direction perpendicular to the main flow. The fluid in the central core region is subjected to a much larger centrifugal force than the region near the wall. Due to the centrifugal force, the fluid in the central core will be pushed toward the outer wall and pressure gradient results throughout the cross-section. For a given Y-coordinate, the pressure is greatest at the outer wall and smallest at the inner wall. For a given X-coordinate to the right of the center of circulation, the pressure is greatest at $Y = 0$ and decreases toward the upper or lower wall. By looking at the secondary flow streamlines, one can also see the distributions of pressure gradients through the cross-section. For example, the strong secondary flow toward the inner wall near the upper or lower wall is caused by large pressure drop whereas the outward flow in the core region is caused by centrifugal forces.

4.3 *The effect of aspect ratio on velocity and temperature fields*

In order to see the effect of aspect ratio on flow and heat transfer characteristics, the aspect ratios $\gamma = 2$, 5, 0·5 and 0·2 are considered in addition to a curved square channel $\gamma = 1$. The effect of the Dean number on velocity and temperature fields in a curved rectangular channel

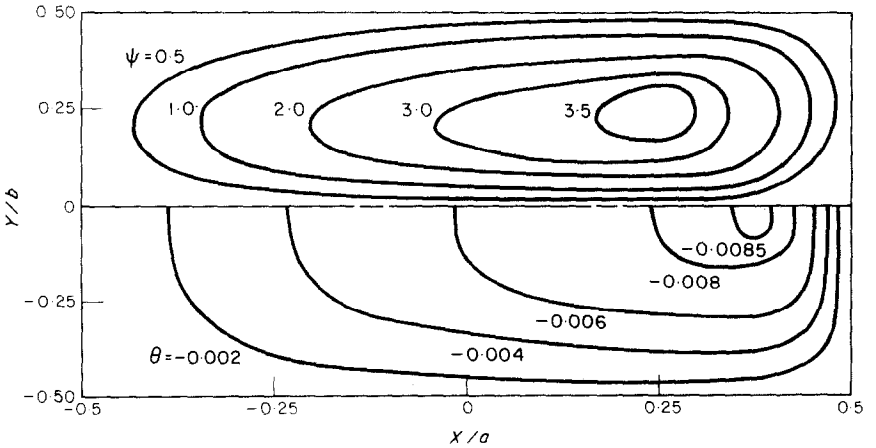

FIG. 6. Secondary flow streamlines and dimensionless isothermals for a curved rectangular channel $\gamma = 2$ with $K = 58{\cdot}8$ and $Pr = 0{\cdot}73$.

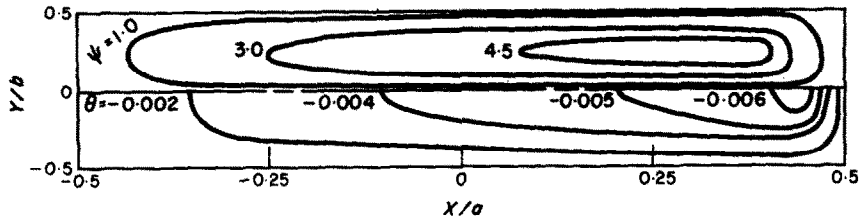

FIG. 7. Secondary flow streamlines and dimensionless isothermals for a curved rectangular channel $\gamma = 5$ with $K = 88{\cdot}1$ and $Pr = 0{\cdot}73$.

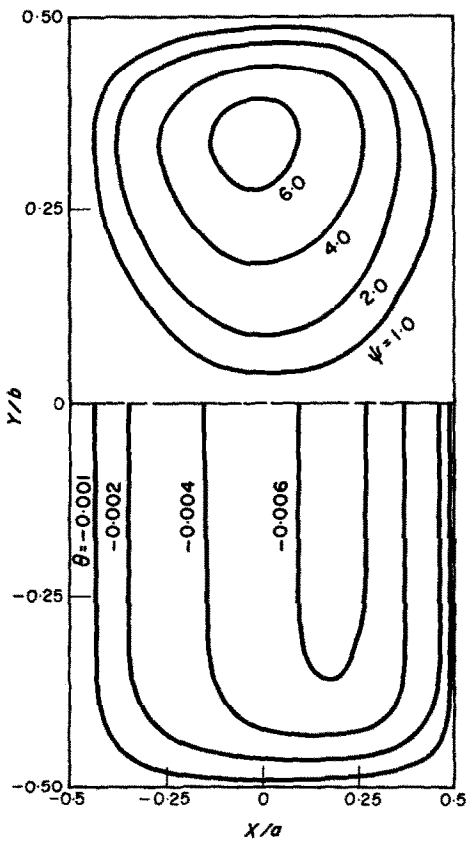

FIG. 8. Secondary flow streamlines and dimensionless isothermals for a curved rectangular channel $\gamma = 0{\cdot}5$ with $K = 103{\cdot}4$ and $Pr = 0{\cdot}73$.

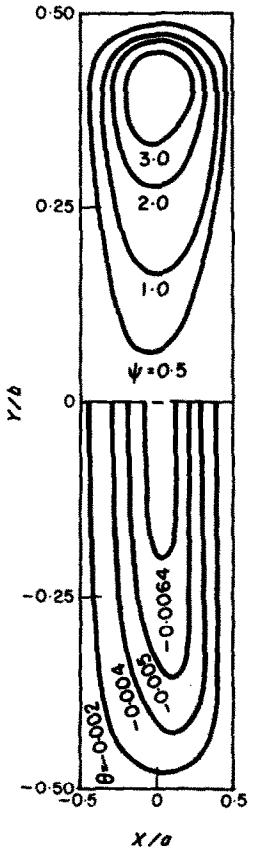

FIG. 9. Secondary flow streamlines and dimensionless isothermals for a curved rectangular channel $\gamma = 0{\cdot}2$ with $K = 79{\cdot}3$ and $Pr = 0{\cdot}73$.

with various aspect ratios is generally similar to that for a curved square channel.

Consider a curved rectangular channel with long side horizontal first. Secondary flow streamlines and isothermals for $\gamma = 2$, Pr = 0·73 and $K = 58{\cdot}8$ are shown in Fig. 6. The center of circulation is fairly close to the outer wall and the secondary motion is weak near the inner wall. This effect is also reflected in the isothermals. For the case $\gamma = 5$ and $Pr = 0{\cdot}73$, the secondary flow streamlines and isothermals for $K = 88{\cdot}1$ are shown in Fig. 7.

The effect of the aspect ratio when the long side is vertical will be examined next. Secondary flow streamlines and isothermals for the aspect ratios $\gamma = 0{\cdot}5$ and 0·2 with $Pr = 0{\cdot}73$ are presented in Figs. 8 and 9, respectively, for representative Dean numbers. With the increase of the Dean number, the center of the circulation tends to move toward the upper or lower horizontal wall. It is not difficult to see the general trend for the velocity and temperature fields with further decrease of the aspect ratio, namely as $\gamma \to 0$. However, one notes that as $\gamma \to 0$, the problem leads to instability problem discussed in [15].

4.4 *The effect of Prandtl number on temperature field*

Observation of the momentum equations (8) and (9) shows that Prandtl number has no effect on the flow field. By comparing the axial momentum equation (9) and the energy equation (10), one notes the similarity between the two equations. In fact if $Pr = 1$, the axial velocity distribution is similar to the temperature distribution for a given Dean number. The effect of inertia terms in equation (9) increases with the increase of the Dean number. Consequently, the effect of Prandtl number on the convective terms of the energy equation (10) is similar to the effect of Dean number on inertia terms in the

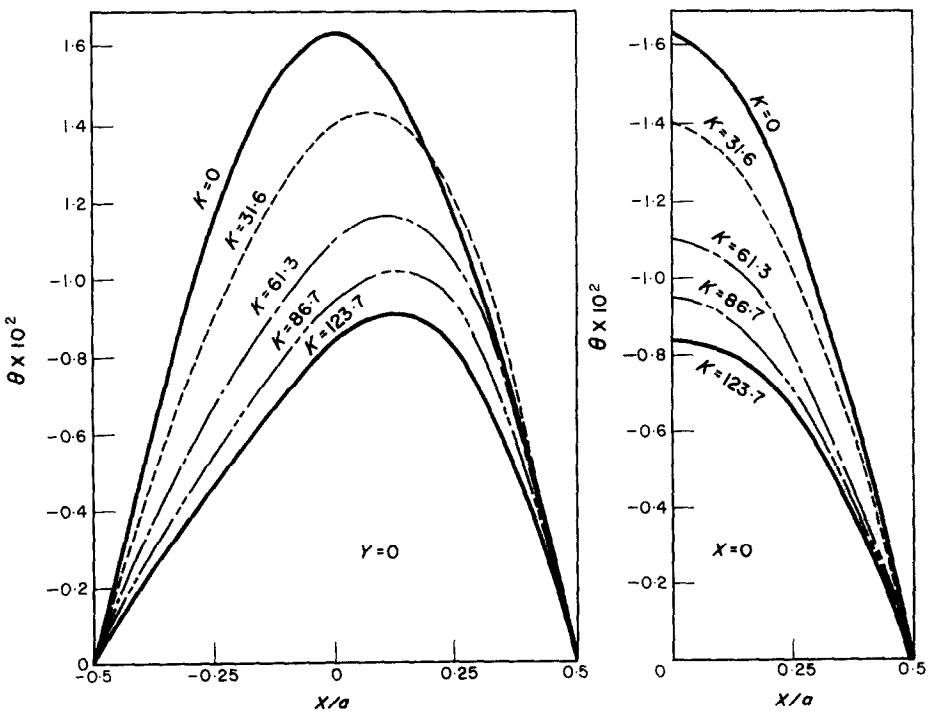

FIG. 10. Dimensionless temperature distribution in a curved square channel $\gamma = 1$ with K as a parameter and $Pr = 0{\cdot}1$.

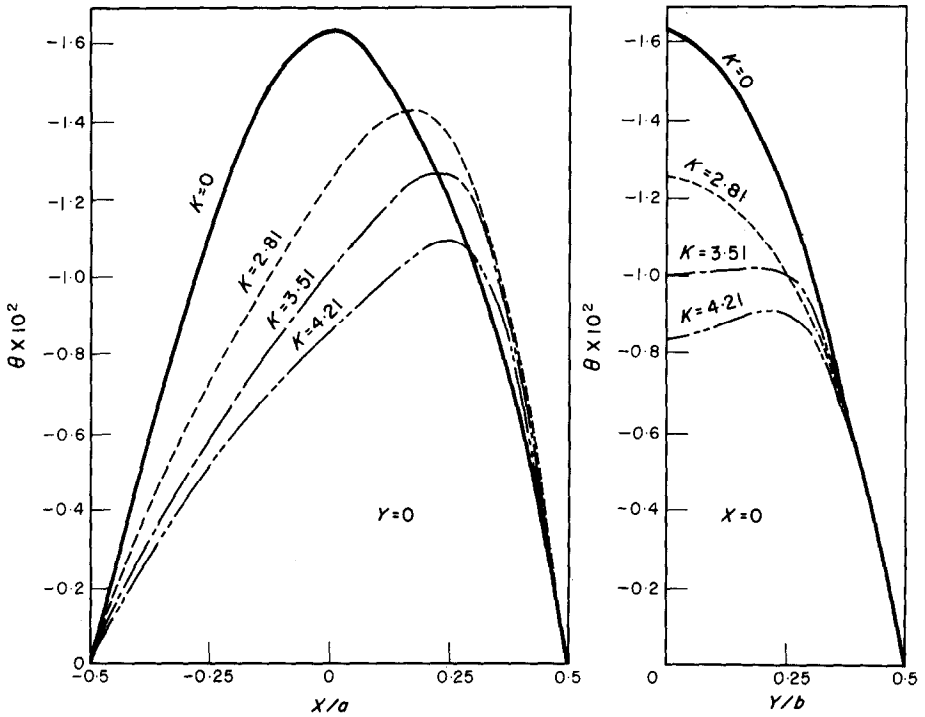

FIG. 11. Dimensionless temperature distribution in a curved square channel $\gamma = 1$ with K as a parameter and $Pr = 10^2$.

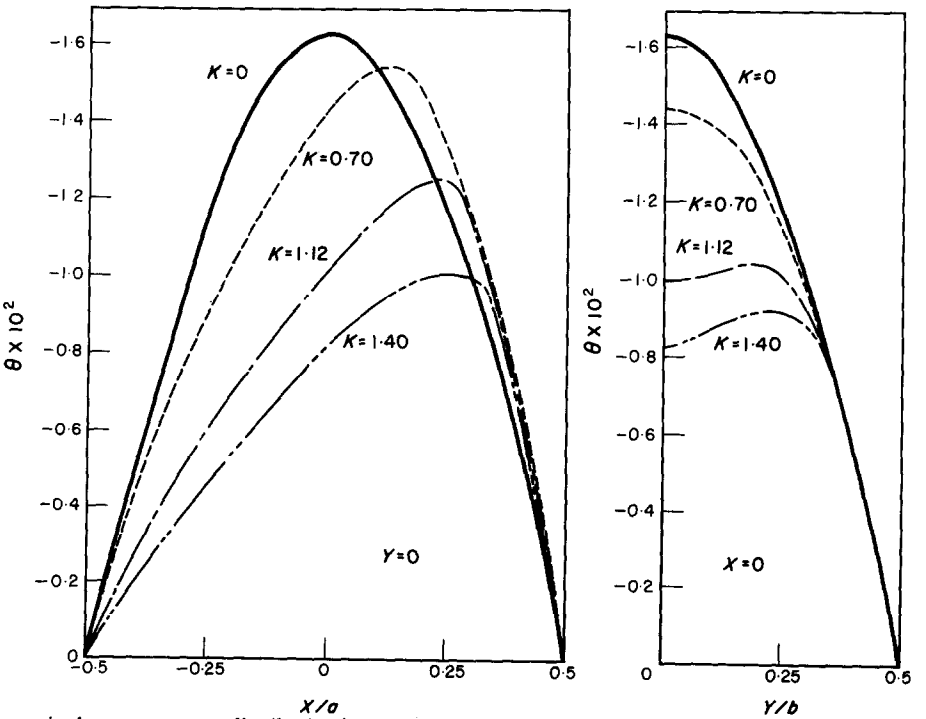

FIG. 12. Dimensionless temperature distribution in a curved square channel $\gamma = 1$ with K as a parameter and $Pr = 10^3$.

momentum equation. Noting the effect of the Dean number on the axial velocity distributions, one can immediately see the effect of Prandtl number on the temperature distributions. The effect of Prandtl number can be seen from Figs. 10 and 12 where temperature distributions through the central axes of a curved square channel $\gamma = 1$ with K as a parameter are shown for $Pr = 0{\cdot}1$, 10^2 and 10^3, respectively.

4.5 *Flow resistance*

The overall flow characteristics will be considered next. The ratio $(f\,Re)/(f\,Re)_0$ between a curved rectangular channel and a straight rectangular channel is plotted against Dean number in Fig. 13 for the aspect ratios $\gamma = 0{\cdot}2$, $0{\cdot}5$, 1, 2 and 5. One sees that for a given axial pressure gradient, the effect of Dean number is greatest for the curved square channel up to $K \approx 100$. It is of interest to note that the aspect ratios $\gamma = 0{\cdot}5$ and 2 represent the same cross-sectional area. Similarly, the cross-sectional area is identical for the aspect ratios $\gamma = 0{\cdot}2$ and 5. Comparison of the curves for $\gamma = 2$ and $0{\cdot}5$ in Fig. 13 shows that the Dean number effect is much stronger for a channel with larger aspect ratio after reaching a certain value of K. Similar remark applies to the cases $\gamma = 5$ and $0{\cdot}2$. This fact is of interest in design. When K is small, the centrifugal force effect is small and the inertia terms may be negligible as compared with the viscous terms. Consequently, the way of placing long side horizontal or vertical has negligible effect on flow resistance. In contrast, for the high Dean number region, the effects of the centrifugal force and inertia terms are significant. The different effect of the aspect ratio with the same cross-sectional area may be explained from the distribution of the centrifugal forces for the high Dean number regime.

The results for the various aspect ratios presented in Fig. 13 show that for the high Dean

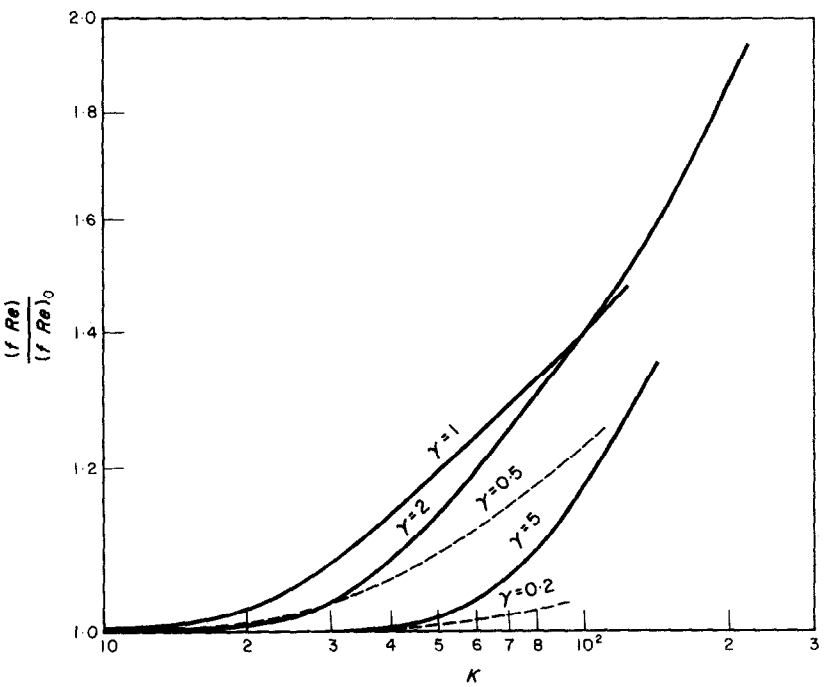

FIG. 13. $(f\,Re)/(f\,Re)_0$ vs. K with aspect ratio γ as a parameter.

number regime, the value of $(fRe)/(fRe)_0$ changes linearly with Dean number K. Consequently, one may write $(fRe)/(fRe)_0 \sim K^m$ where m depends on aspect ratio. For example,

$$(fRe)/(fRe)_0 \approx 0{\cdot}225K^{0{\cdot}39}$$

$$\text{for } \gamma = 1 \text{ and } 10^2 < K < 1{\cdot}5 \times 10^3.$$

Comparison of the result from the present analysis for curved square channel with the results available in the literature is of considerable interest and is shown in Fig. 14. One can see that the present study covers the Dean number ranging from small to a reasonably high region where no other work is available in the literature. One numerical datum at a quite high Dean number is also plotted in Fig. 14 for comparison and shows a very good agreement with Ludwieg's experimental data [6]. Mori and Uchida's analysis [14] using boundary layer approximation for the high Dean number agrees well with Ludwieg's experimental data up to a certain Dean number. Beyond that the experimental data by Ludwieg are suspected to be in the turbulent region. The two curves given by Mori and Uchida represent the first and second approximations.

Observation of the result from the present numerical analysis and the results from Ludwieg [6] and Mori and Uchida [14] for curved square channel shows clearly that a reasonable estimate can be made for the flow resistance with the Dean number ranging from 150 to 1000 where currently accurate analytical solution is not available.

4.6 *Heat transfer*

The overall heat transfer characteristics will be examined next. The graphical results for the Nusselt number ratio $Nu/(Nu)_0$ versus Dean number are shown in Fig. 15 for the aspect ratios $\gamma = 0{\cdot}2, 0{\cdot}5, 1, 2$ and 5 with $Pr = 0{\cdot}73$. As noted earlier, the effect of Prandtl number on temperature field is considerable. This is also reflected in heat transfer results shown in Fig. 16 where $Nu/(Nu)_0$ is plotted against K for a curved

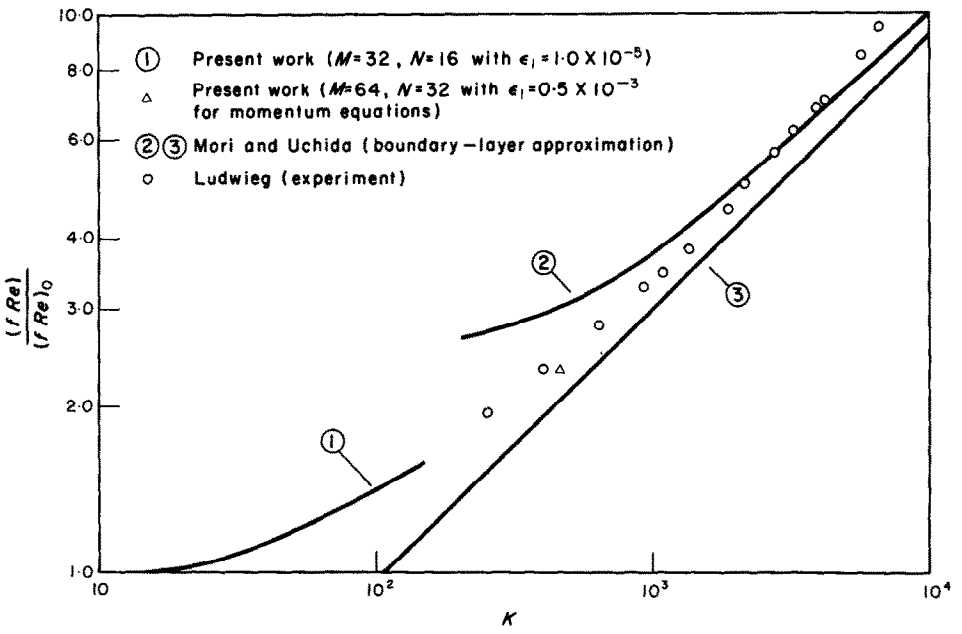

FIG. 14. Comparison of the results for friction factor from this work with the theoretical and experimental results available in literature ($\gamma = 1$).

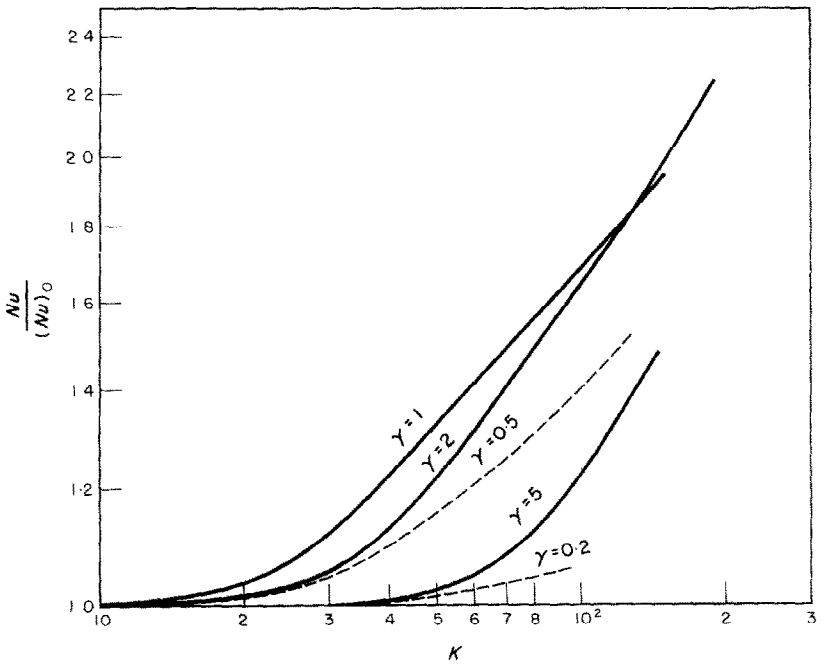

FIG. 15. $(Nu)/(Nu)_0$ vs. K with aspect ratio γ as a parameter and $Pr = 0{\cdot}73$.

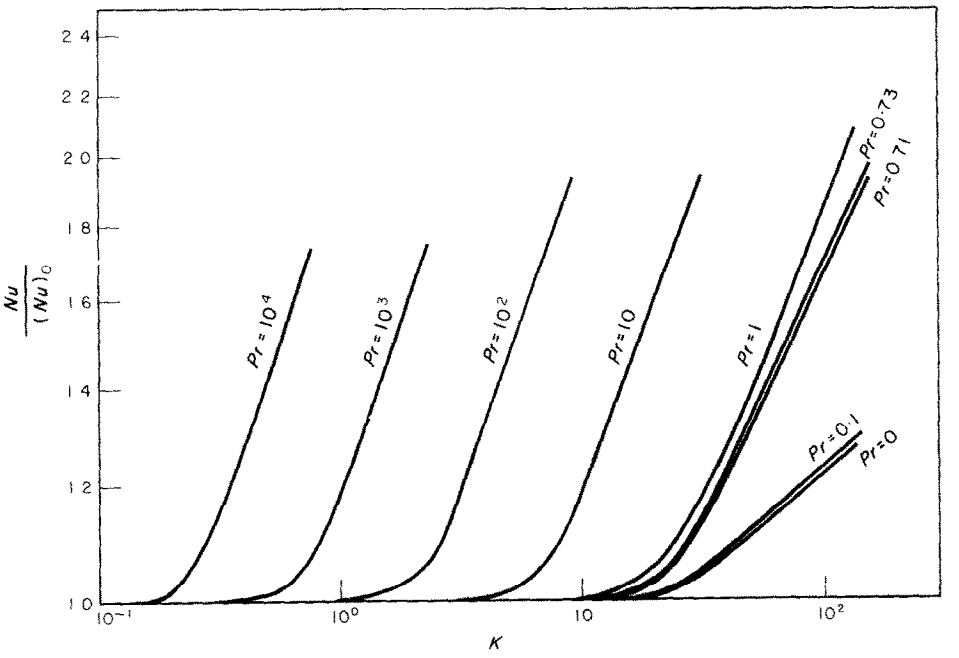

FIG. 16. $(Nu)/(Nu)_0$ vs. K with Prandtl number Pr as a parameter in a curved square channel $\gamma = 1$.

square channel with $Pr = 0, 0{\cdot}1, 0{\cdot}71, 0{\cdot}73, 1, 10, 10^2, 10^3$ and 10^4. It is seen that an asymptotic line exists for the heat transfer result too in the high Dean number region for a given Prandtl number. The following approximate expression may be used for the high Dean number regime.

$$Nu/(Nu)_0 = 0{\cdot}182K^{\frac{1}{2}}Pr^{\frac{1}{2}}$$

$$\text{for } 1 \leqslant Pr \leqslant 10^4, \gamma = 1 \text{ and } Nu/(Nu)_0 \leqslant 1{\cdot}5.$$

It is of interest to note that, for example, at $Nu/(Nu)_0 = 1{\cdot}6$ the distance between two neighboring curves decreases slightly as Pr increases by the same factor.

The heat transfer result from the present analysis is compared with the result from Mori and Uchida [14] in Fig. 17 for a curved square channel $\gamma = 1$. Mori and Uchida [14] show the first and second approximations for the ratio of Nusselt numbers for $Pr = 0{\cdot}71$ and ∞. A datum from numerical solution at $K = 460$ is also shown in the figure for comparison. Considering the case $Pr = 0{\cdot}71$, one sees that the present result is very reasonable up to a fairly high Dean number and suggests clearly that a reasonable estimate can be made for the Dean number ranging from $K = 150$ to 1000 as shown as a broken line in Fig. 17.

Mori and Uchida's work [14] shows that an asymptotic value exists for the ratio $Nu/(Nu)_0$ as $Pr \to \infty$. However, the numerical result from this study shows that an asymptotic line for $Pr = \infty$ will not be reached at least up to the range ($Pr = 10^4$) studied in this work. Furthermore, in [22] it is stated that the Nusselt number ratio approaches the asymptotic value with the increasing Prandtl number for a similar problem in curved pipes. Based on the result of this work, it appears that an asymptotic value does not exist at least up to $Pr = 10^4$. On the other hand, an asymptotic value does exist for $Pr \to 0$.

It is known that as the Dean number increases, the effect of the convective terms in the energy equation (10) increases for a given Prandtl number. As the Prandtl number increases, the effect of the convective terms also increases for a given Dean number. One can see that the Nusselt number increases with the increase of the Prandtl number even if the Dean number is held constant. The effect of the Prandtl number is equivalent to the effect of the Dean number. For example, at $Nu/(Nu)_0 = 1{\cdot}6$, as the Prandtl number increases from 10 to 10^3, the Dean

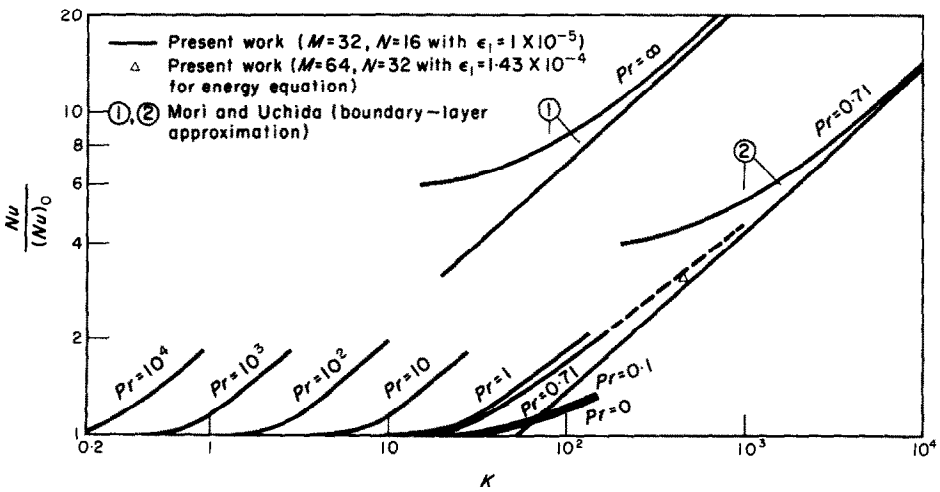

FIG. 17. Comparison of heat transfer results from this work with theoretical results available in literature for $\gamma = 1$.

number decreases from $K \approx 20$ to $K \approx 2$. The numerical results based on two different methods of obtaining flow and heat transfer results discussed in Section 4.1 show that the two methods are off by only 0·4 per cent at most for all the cases considered. This confirms the accuracy of the numerical solutions. From equations (18) and (20), one sees that

$$\left(\frac{\partial \overline{w}}{\partial n}\right)_w = 1 \text{ and } \left|\frac{\partial \overline{\theta}}{\partial n}\right|_w = \frac{\overline{w}}{4}.$$

The numerical results check excellently with the above relations confirming again the accuracy of the numerical solution. The complete numerical results for flow and heat transfer as well as velocity and temperature profiles for the cases other than $\gamma = 1$ are given in [2].

5. CONCLUDING REMARKS

1. Numerical solution by point successive-over relaxation is obtained for laminar forced convection in curved rectangular channels with various aspect ratios for a range of Dean numbers shown in Figs. 13 and 15. The limitation of the numerical method is encountered at a reasonably high Dean number. The difficulty seems to come from the non-linear terms in the equations and the fact that viscous term and conduction term can be neglected in the core region at high Dean number. In spite of this difficulty the numerical method has definite advantage over the perturbation method [24].

2. By using $\omega = 1$ for the relaxation factor in the high Dean number region, the range of the numerical solution in terms of the ratios $(fRe)/(fRe)_0$ and $Nu/(Nu)_0$ is further extended beyond the range studied in [20]. For a curved rectangular channel with $\gamma = 2$ the numerical solution is obtained up to the ratios $(fRe)/(fRe)_0 = 1{\cdot}8$ and $Nu/(Nu)_0 = 2{\cdot}2$, respectively. One sees that the range of applicability of the present numerical solution far exceeds that of the perturbation method for curved pipe [24]. The numerical method is effective for the flow regime with Dean number ranging from small to a reasonably high value and complements the boundary layer technique [14].

3. The effect of Prandtl number on heat transfer result is significant. The effect of the Prandtl number is equivalent to that of Dean number. It is pointed out in References [14, 22] that the Nusselt number ratio $Nu/(Nu)_0$ approaches the asymptotic value as the Prandtl number approaches infinity. The result of this analysis shows that the asymptotic line for $Pr = \infty$ will not be reached at least up to $Pr = 10^4$. In [22] the heat transfer results obtained from boundary layer approximation for $Pr = \infty$ are shown to agree with the experimental results obtained by Seban and McLaughlin [23] for $Pr \approx 400$. Based on the result of this analysis it is believed that the asymptotic line for $Pr = \infty$ obtained by boundary-layer approximation may lead to some error in heat transfer prediction when $Pr > 400$. On the other hand, as $Pr \to 0$, the heat transfer result approaches the asymptotic value as shown in Figs. 16 and 17. One may note that the boundary-layer approximation cannot be used as $Pr \to 0$.

4. Comparison of the results from this analysis and the results available in the literature [6, 14] for a curved square channel shows that a reasonable estimate can be made for the flow and heat transfer results for the Dean number ranging from 150 to 1000 where currently accurate solutions are not available.

5. The result of this analysis confirms the known fact that the local heat transfer coefficient is higher at the outer wall of the curved channel than at the inner wall.

6. It may be worthwhile to point out that the assumption 1 in the formulation of the problem was introduced to limit the scope of the present investigation. The order of magnitude analysis for the fundamental equations for the curved channel flow [2] shows that another independent dimensionless parameter (D_e/R_c) representing the curvature effect is required for the case when the radius of curvature of the channel is not large as compared with D_e. The inclusion of the

curvature parameter D_e/R_c in the analysis leads to more terms such as Coriolis force term in the governing equations. One may add that under certain conditions the buoyancy force effect on forced convection heat transfer in curved channels cannot be neglected [2].

7. The convergence of the numerical solution is ascertained by comparing the numerical results using two methods of evaluating fRe and Nu. Comparison of the numerical results with the known exact values for the limiting case of straight channel ($K = 0$) shows excellent agreement also. Some details on the quantitative evaluation of the degree of convergence are given in [2]. The important question of whether the numerical computations converge to the physical solution can be answered only partially by the rather good agreement of one numerical datum with Ludwieg's experimental data as shown in Fig. 14. Similar comparison for the heat transfer results is not possible at present due to the lack of experimental data. However, it is known that Nusselt number results should show the same trend as the friction factor results.

ACKNOWLEDGEMENT

This work was supported by the National Research Council of Canada through Grant NRC A-1655. The authors wish to thank Miss Lynne Fiveland for her excellent typing of the manuscript.

REFERENCES

1. L. Trefethen, Fluid flow in radial rotating tubes, *Actes, IX^e Congrès International de Méchanique Appliqueé*, Vol. 2, Université de Bruxelles, 341–350 (1957).
2. M. Akiyama, Laminar forced convection heat transfer in curved rectangular channels, M.Sc. thesis, Mechanical Engineering Department, University of Alberta, Edmonton, Alberta, Canada (1969).
3. H. Ito, Theory on laminar flows through curved pipes of elliptic and rectangular cross-sections, The Reports of the Institute of High Speed Mechanics, Tohoku University, Sendai, Japan, Vol. 1, 1–16 (1951).
4. H. G. Cuming, The secondary flow in curved pipes, Aeronautical Research Council, Reports and Memoranda, No. 2880 (1952).
5. W. R. Dean and J. M. Hurst, Note on the motion of fluid in a curved pipe, *Mathematika* **6**, 77–85 (1959).
6. H. Ludwieg, Die ausgebildete kanalströmung in einem rotierenden system, *Ingenieur-Archiv* **19**, 296–308 (1951).
7. H. P. Eichenberger, Secondary flow within a bend, *J. Math. Phys.* **32**, 34–42 (1953).
8. J. N. Kapur, V. P. Tyagi and R. C. Srivastava, Streamline flow through a curved annulus, *Appl. Scient. Res.* **A14**, 253–267 (1964).
9. H. C. Topakoglu, Steady laminar flows of an incompressible viscous fluid in curved pipes, *J. Math. Mech.* **16**, 1321–1337 (1967).
10. F. L. Wattendorf, A study of the effect of curvature on fully developed turbulent flow, *Proc. R. Soc.* **148**, 565–598 (1935).
11. S. Eskinazi and H. Yeh, An investigation on fully developed turbulent flows in a curved channel, *J. Aeronaut. Sci.* **23**, 23–34, 75 (1956).
12. F. Kreith, The influence of curvature on heat transfer to incompressible fluids, *Trans. Am. Soc. Mech. Engrs* **77**, 1247–1256 (1955).
13. B. P. Ustimenko, K. A. Zhurgembaer and D. A. Nusupbekova, Calculation of convective heat transfer for an incompressible liquid in complex-configuration channels, *Proc. Second All-Soviet Union Conf. Heat Mass Transfer* **1**, 124–143 (1966).
14. Y. Mori and Y. Uchida, Study on forced convective heat transfer in curved square channel (1st report. Theory of laminar region), *Trans. Japan Soc. Mech. Engrs* **33**, 1836–1846 (1967).
15. Y. Mori and Y. Uchida, Forced convective heat transfer in a curved channel, *JSME* 1967 *Semi-Int. Symp., Heat and Mass Transfer, Thermal Stress* **1**, 181–190 (1967).
16. J. O. Wilkes and S. W. Churchill, The finite-difference computation of natural convection in a rectangular enclosure, *A.I.Ch.E.Jl* **12**, 161–166 (1966).
17. M. R. Samuels and S. W. Churchill, Stability of a fluid in a rectangular region heated from below, *A.I.Ch.E.Jl* **13**, 77–85 (1967).
18. H. Z. Barakat and J. A. Clark, Analytical and experimental study on the transient laminar natural convection flows in partially filled liquid containers, *Proc. Third Int. Heat Transfer Conf. A.I.Ch.E.* **2**, 152–162 (1966).
19. G. de Vahl Davis, Laminar natural convection in an enclosed rectangular cavity, *Int. J. Heat Mass Transfer* **11**, 1675–1693 (1968).
20. K. C. Cheng and G. J. Hwang, Numerical solution for combined free and forced laminar convection in horizontal rectangular channels, *J. Heat Transfer*, **91**, 59–66 (1969).
21. D. Young, The numerical solution of elliptic and parabolic partial differential equations, *Survey of Numerical Analysis*, edited by J. Todd, pp. 380–438. McGraw-Hill, New York (1962).
22. Y. Mori and W. Nakayama, Study on forced convective heat transfer in curved pipes (1st report. Laminar region). *Int. J. Heat Mass Transfer* **8**, 67–82 (1965).
23. R. A. Seban and E. F. McLaughlin, Heat transfer in tube coils with laminar and turbulent flow, *Int. J. Heat Mass Transfer* **6**, 387–395 (1963).
24. M. N. Özisik and H. C. Topakoglu, Heat transfer for laminar flow in a curved pipe, *J. Heat Transfer* **90**, 313–318 (1968).

CONVECTION FORCÉE LAMINAIRE DANS DES CONDUITES RECTANGULAIRES COURBES

Résumé—Le but de cet article est de présenter des résultats d'écoulement et de transport de chaleur obtenus par une méthode de surrelaxation ponctuelle successive pour un écoulement laminaire permanent entièrement établi dans des conduites rectangulaires courbes sous les conditions aux limites thermiques d'un flux de chaleur pariétal uniforme axialement et d'une température pariétale uniforme périphériquement à n'importe quelle position axiale. La méthode numérique fournit des solutions jusqu'à un nombre de Dean raisonnablement élevé pour les allongements = 0,2, 0,5, 1, 2 et 5 considérés dans cette étude. On a remarqué que la méthode des perturbations est appliquable seulement pour la région des nombres de Dean relativement bas et que la technique de la couche limite est valable seulement pour le régime des nombres de Dean élevés.

Les résultats respectivement pour $f\,Re/(f\,Re)_0$ et $Nu/(Nu)_0$ sont présentés graphiquement en fonction du nombre de Dean pour $Pr = 0{,}73$. On montre également des exemples typiques pour les profils de vitesse axiale et de température, les lignes de courant et les profils de vitesse pour l'écoulement secondaire et les isothermes.

Pour la conduite de section carrée, l'effet du nombre de Prandtl sur le résultat du transport de chaleur est aussi étudié. La comparaison du résultat à partir de cette analyse et le résultat, pour le régime des nombres de Dean élevés dans la conduite carrée courbe, disponible dans la littérature, montre clairment qu'une estimation raisonnable peut être faite pour les résultats d'écoulement et de transport de chaleur pour le nombre de Dean allant de 150 à 1000 où des solutions généralement précises ne sont pas disponibles.

LAMINARE, ERZWUNGENE KONVEKTION IN GEKRÜMMTEN RECHTECKKANÄLEN

Zusammenfassung—In vorliegender Arbeit werden Ergebnisse für die Strömung und den Wärmeübergang gebracht, die nach einer punktweisen Überrelaxationsmethode für stationäre voll ausgebildete Laminarströmung in gekrümmten Rechteckkanälen bei achsial einheitlichem Wärmestrom durch die Wand und bei peripher einheitlicher Wandtemperatur in beliebiger achsialer Lage erhalten wurden. Die numerische Methode liefert Lösungen bis zu einer ziemlich hohen Dean-Zahl für Anordnungsverhältnisse von = 0·2, 0·5, 1, 2, und 5 wie sie hier zugrundegelegt sind. Es sei bemerkt, dass die Perturbationsmethode nur für relativ niedrige Dean-Zahlbereiche anwendbar ist und die Grenzschichttechnik nur für hohe Dean-Zahlen gültig ist. Für $Pr = 0{\cdot}73$ ist $f(Re)/f\,(Re)_0$ bzw. Nu/Nu_0 in Abhängigkeit von der Dean-Zahl grafisch wiedergegeben. Typische Beispiele für Achsialgeschwindigkeit und Temperaturprofile, Stromlinien und Geschwindigkeitsprofile für Sekundärströmung und Isothermen werden ebenfalls gezeigt. Für Rechteckkanäle wird auch der Einfluss der Prandtl-Zahl auf den Wärmeübergang untersucht. Ein Vergleich aus dem Ergebnis dieser Analyse und dem Ergebnis für einen hohen Dean-Zahlbereich zeigt deutlich, dass vernünftige Abschätzungen für die Strömung und den Wärmeübergang für Dean-Zahlen von 150 bis 1000 gemacht werden können, wo gegenwärtig keine genauen Lösungen verfügbar sind.

ЛАМИНАРНАЯ ВЫНУЖДЕННАЯ КОНВЕКЦИЯ В ИСКРИВЛЕННЫХ ПРЯМОУГОЛЬНЫХ КАНАЛАХ

Аннотация—В данной статье представлены результаты по исследованию теплообмена релаксационным методом в развитом ламинарном потоке в искривленных прямоугольных каналах при двух типах граничных условий: а) равномерно распределенный на стенке осевой тепловой поток; б) одинаковая по периметру в любом осевом сечении температура стенки. Численным методом получены решения для больших чисел Дина при соотношениях сторон, равных 0,2; 0,5; 1,2 и 5. Отмечается, что метод возмущений применим только для относительно малых чисел Дина, тогда как приближение пограничного слоя справедливо только для больших значений числа Дина.

Приводятся зависимости $fRe/(fRe)_0$ и $Nu/(Nu)_0$ от числа Дина при $Pr = 0{,}73$. Приведены характерные распределения температуры и скорости по оси, изотермы, профили скорости и линии тока при вторичном течении. Кроме того, в канале квадратного сечения исследовалось влияние на теплообмен числа Прандтля. Из сравнения полученных результатов и имеющихся данных вытекает, что в криволинейном канале квадратного сечения можно рассчитать гидродинамику и теплообмен в диапазоне изменения чисел Дина от 150 до 1000, для которого еще нет точного решения.